



1 **Multiproxy evidence of the Neoglacial expansion of Atlantic**
2 **Water to eastern Svalbard: Does ancient environmental DNA**
3 **complement sedimentary and microfossil records?**

4
5 Joanna Pawłowska^{1*}, Magdalena Łacka¹, Małgorzata Kucharska¹, Jan Pawłowski², Marek
6 Zajączkowski¹

7
8 ¹Institute of Oceanology Polish Academy of Sciences, Sopot, 81-712, Poland

9 ²Department of Genetics and Evolution, University of Geneva, Geneva, CH 1211, Switzerland

10 *Correspondence to:* Joanna Pawłowska (pawlowska@iopan.pl)

11

12

13 **Abstract.** The main goal of this study was to reconstruct the paleoceanographic development
14 of Storfjorden during the Neoglacial (~ 4 cal ka BP). A multiproxy approach was applied to
15 provide evidence for interactions between the inflow of Atlantic Water (AW) and sea-ice
16 coverage, which are the major drivers of environmental changes in Storfjorden. The
17 sedimentary and microfossil records indicate that a major reorganization of oceanographic
18 conditions in Storfjorden occurred at ~ 2.7 cal ka BP. A general cooling and the less
19 pronounced presence of AW in Storfjorden during the early phase of the Neoglacial are
20 prerequisite conditions for the formation of an extensive sea-ice cover. The period after ~ 2.7
21 cal ka BP was characterized by alternating short-term cooling and warming intervals.
22 Warming was associated with pulsed inflows of AW and sea-ice melting that stimulated
23 phytoplankton blooms and organic matter supply to the bottom. The cold phases were
24 characterized by heavy and densely packed sea ice resulting in a decrease in productivity. The
25 ancient environmental DNA (aDNA) records of foraminifera and diatoms reveal the timing of
26 the major pulses of AW (~2.3 and ~1.7 cal ka BP) and the variation in sea-ice cover. The AW
27 inflow was marked by an increase in the percentage of DNA sequences of monothalamous
28 foraminifera associated with the presence of fresh phytodetritus, while cold and less
29 productive intervals were marked by an increased proportion of monothalamous taxa known
30 only from environmental sequencing. The diatom aDNA record indicates that primary
31 production was continuous during the Neoglacial regardless of sea-ice conditions. However,



1 the colder periods were characterized by the presence of diatom taxa associated with sea ice,
2 whereas the present-day diatom assemblage is dominated by open-water taxa.

3

4 **1. Introduction**

5 The flow of Atlantic Water (AW) is one of the major heat contributors to the Arctic
6 Ocean (Polyakov et al., 2017). Recent oceanographic data indicate warming due to an
7 increase in AW in the Arctic Ocean (Rudels et al., 2015, Polyakov et al., 2017). AW has been
8 present along the western margin of Svalbard during at least the last 12,000 years (e.g.,
9 Werner et al., 2011; Rasmussen et al., 2014). One of the major intrusions of AW occurred
10 during the early Holocene (10.8 – 6.8 cal ka BP). A distinct cooling and freshening of the
11 bottom water masses occurred during the mid-late Holocene (6.8–1 cal ka BP) and was
12 accompanied by glacier readvances in Svalbard leading to present-day conditions
13 (Ślubowska-Woldengen et al., 2007; Telesiński et al., 2018). The paleoceanographic
14 conditions in the Svalbard margins correlate closely to the sea surface temperature (SST)
15 variations in the Nordic Seas and confirm that the Svalbard area is highly sensitive to
16 fluctuations in the inflow of AW (Ślubowska-Woldengen et al., 2007). Conversely, until the
17 1990s eastern Svalbard was recognized as an area exclusively influenced by the East
18 Spitsbergen Current (ESC), which carries cold and less saline Arctic Water (ArW) from the
19 Barents Sea (e.g., Quadfasel et al., 1988; Piechura et al., 1996). Recent studies have revealed
20 that the oceanography of the area is much more complicated (e.g. Skogseth et al., 2007; Geyer
21 et al., 2010). Oceanographic data obtained from conductivity–temperature sensors attached to
22 *Delphinapterus leucas* show a substantial contribution of AW to Storfjorden (east
23 Spitsbergen; Lydersen et al., 2002). Recently, a suggestion by Hansen et al. (2011) that AW
24 was present in Storfjorden during the early Holocene warming (11 – 6.8 cal ka BP) was
25 confirmed by Łącka et al. (2015). However, the limited amount of data available for eastern
26 Svalbard often makes paleoceanographic reconstructions of the area speculative.

27 The latter part of the Holocene, the so-called Neoglacial cooling (~ 4 cal ka BP), in the
28 European Arctic is correlated with a decline in the summer insolation at northern latitudes
29 (Berger, 1978) and a decline in summer SST (Andersen et al., 2004; Risebrobakken et al.,
30 2010; Rasmussen et al., 2014). The cooling of the surface waters and the limited AW inflow
31 to the Nordic Seas led to the formation of an extended sea-ice cover (Müller et al., 2012). In
32 addition, the southwestern and eastern shelf of Spitsbergen experienced a strengthening of the
33 East Spitsbergen Current leading to an intensification of ArW inflow and the formation of an
34 extensive sea-ice cover (Sarnthein et al., 2003). Therefore, the Neoglacial has usually



1 considered a constantly cold period, with a culmination of cooling during the Little Ice Age.
2 However, the records from Storfjorden and the Barents Sea suggest that the Neoglacial was a
3 period of variable oceanographic conditions with strong temperature and salinity gradients
4 (Calvo et al., 2002; Martrat et al., 2003; Sarnthein et al., 2003; Łącka et al., 2015). There is
5 also evidence of episodic intensifications of the warm AW inflow to western Svalbard at that
6 time (e.g. Risebrobakken et al. 2010; Rasmussen et al., 2012).

7 According to Nilsen et al. (2008), the critical parameter controlling the fjord–shelf
8 exchange is the density difference between the fjord water masses and the AW. The local
9 winter ice production and formation of brine-enriched waters determines the density of local
10 water masses, which is a key factor that enables AW to penetrate into fjords during the spring
11 and summer. Moreover, the production of brine-enriched waters and associated deep-water
12 overflow is a key contributor to large-scale ocean circulation (Killworth, 1983). In this
13 respect, Storfjorden is especially important because it is one of the few areas where brine-
14 enriched waters have been frequently observed (Haarpainter et al., 2001). In the last decades,
15 reduced brine formation occurred during periods with the most intensive AW advection to
16 Storfjorden and reduced sea-ice formation in the Barents Sea, while intense brine formation
17 was re-established during periods of recurrent cooling (Årthun et al., 2011).

18 The aim of the presented study is to reconstruct the paleoceanographic development of
19 Storfjorden during the Neoglacial with multicentennial resolution. We assumed that the
20 periodic intensification of the AW inflow to the West Spitsbergen shelf during the Neoglacial
21 resulted in the appearance of AW also in eastern Spitsbergen, similar to the early Holocene
22 (e.g., Łącka et al., 2015), affecting the density and extent of sea-ice cover in the area. A
23 multiproxy approach comprising composed of sedimentary, microfossil and molecular records
24 was applied to provide evidence for interactions between the inflow of AW and sea-ice
25 coverage in Storfjorden. The ancient environmental DNA (aDNA) analysis targeted diatoms
26 and nonfossilized monothalamous foraminifera, groups that are hardly preserved in fossil
27 records from the Spitsbergen fjords (Pawłowska et al., 2014, Łącka M., *pers. commun.*)
28 Recent studies have demonstrated that analyses of genetic material obtained directly from
29 environmental samples (so called environmental DNA) are an efficient method for
30 biodiversity surveys across time and space (Thomsen and Willerslev, 2015). Our previous
31 studies of foraminiferal aDNA revealed the extraordinary richness of the foraminiferal
32 community, primarily due to the detection of soft-walled monothalamous taxa (Pawłowska et
33 al., 2014). Furthermore, aDNA has been proven to be an effective tool in paleoceanographic
34 reconstructions (e.g. Boere et al., 2009; Pawłowska et al., 2016). The molecular data



1 correlated well with environmental changes and even revealed small changes that were not
2 clearly indicated by other proxy records (Pawłowska et al., 2016). The combination of aDNA
3 studies with the analysis of microfossils and sedimentary proxies provides a powerful means
4 to reconstruct past environments more comprehensively.

5

6 **2. Study area**

7 Storfjorden is located in southeastern Svalbard between the islands of Spitsbergen,
8 Edgeøya and Barentsøya. Storfjorden is ~190 m long and its main basin is ~190 m deep. Two
9 narrow and shallow passages Heleysundet and Freemansundet connect northern Storfjorden to
10 the Barents Sea. To the south, a 120-m-deep sill separates the main basin from the
11 Storfjordrenna Trough. Storfjordrenna is 245 m long, with a depth varying from 150 m to 420
12 m.

13 The water masses in Storfjorden are composed primarily of exogenous Atlantic and
14 Arctic waters and mixed waters that have formed locally. Warm AW is transported by the
15 West Spitsbergen Current branches off near Storfjordrenna and enters the southern part of the
16 fjord. Arctic water (ArW) from the Arctic Ocean and the Barents Sea enters Storfjorden via
17 two passages to the northeast and continues along the inner shelf of Svalbard as a coastal
18 currents. AW is characterized by temperatures > 3 °C and salinity > 34.95 , while the
19 temperature and salinity of ArW are < 0 °C and 34.3-34.8, respectively. The presence of
20 locally formed water masses is a result of the interactions between AW, ArW and melt water.
21 Skogseth et al. (2005) listed six local water masses: melt water (MW), polar front water (PW),
22 East Spitsbergen water (ESW), brine-enriched shelf water (BSW), Storfjorden surface water
23 (SSW), and modified Atlantic water (MAW). BSW is formed due to the release of large
24 amounts of brines during polynya events and the intensive formation of sea ice (Haarpainter
25 et al., 2001; Skogseth et al., 2004, 2005) and is characterized by salinities exceeding 34.8 and
26 temperatures below -1.5 °C (Skogseth et al., 2005).

27 The sedimentary environment in Storfjorden classified as a low-energy, high-
28 accumulation environment, characteristic of inner fjords. The area is sheltered from along-
29 shelf bottom currents and is affected by high terrigenous inputs; therefore deposition prevails
30 over sediment removal by bottom currents (Winklemann and Knies, 2005). The primary
31 productivity is high and strongly depends on the sea ice formation and the duration of the
32 marginal ice zone (Winkelman and Knies, 2005).

33

34



1 **3. Materials and methods**

2 **3.1 Sampling**

3 The 55-cm-long sediment core ST_1.5 was taken with a gravity corer in Storfjorden
4 during cruise of the R/V *Oceania* in August 2014. The sampling station was located at 76°
5 53,181' N and 19° 27,559' E at a depth of 153 m (Fig. 1). The core was stored at 4°C and
6 shipped to the Institute of Oceanology PAS for further analyses.

7 In the laboratory, the core was extruded and cut into 1-cm slices. During cutting,
8 sterile subsamples for ancient DNA (aDNA) analyses were taken at 5 cm intervals. To avoid
9 extraneous and/or cross-contamination the thin layers of sediment that were in contact with
10 under- or overlying sediments were removed using a sterile spatula. Samples for aDNA
11 analyses were taken every 5 cm and kept frozen in -20°C.

12

13 **3.2 Sediment dating**

14 The chronology of the sediment layers is based on high-precision accelerator mass
15 spectrometry (AMS) ¹⁴C dating performed on five bivalve shells from the sediment layers at
16 2.5, 5.5, 14.5, 43.5, 52.5 cm. The shells were identified to the highest possible taxonomic
17 level and processed on the 1.5 SDH-Pelletron Model “Compact Carbon AMS” in the Poznań
18 Radiocarbon Laboratory, Poznań, Poland. The dates were converted into calibrated ages using
19 the calibration program CALIB Rev. 6.1.0 Beta (Stuiver and Reimer, 1993) and the Marine13
20 calibration dataset (Reimer et al., 2013). A difference (ΔR) in the reservoir age correction of
21 105 ± 24 was applied (Mangerud et al., 2006). The calibrated results are reported in units of
22 thousand calibrated years BP (cal ka BP), see Table 1.

23

24 **3.3 Sediment grain size**

25 Samples for the grain size analyses were freeze-dried and milled. Measurements were
26 performed using a Mastersizer 2000 particle laser analyzer coupled to a Hydro MU device
27 (Malvern, UK). Samples were treated with ultrasound to avoid aggregation. Raw data were
28 analyzed using GRADISTAT v.8.0 software (Blott and Pye, 2001). The mean 0-63- μ m grain
29 size [ϕ] was calculated via the logarithmic method of moments. The sediment fraction >500
30 μ m was used for an ice rafted debris (IRD) analysis. Grains were counted under a
31 stereomicroscope and the amount of IRD is reported as the number of grains per gram of dry
32 sediment [grains g⁻¹] and flux [grains cm⁻² y⁻¹].

33

34



1 **3.4 Fossil foraminifera**

2 Prior to fossil foraminifera analysis, samples were wet sieved through a mesh with
3 500- μm and 100- μm openings and dried at 60°C. Samples with large quantities of tests were
4 divided using a microsplitter. At least 300 specimens of benthic foraminifera were isolated
5 from each sample and collected on micropaleontological slides. Benthic foraminifera
6 specimens were counted and identified to the lowest possible taxonomic level. The quantity of
7 foraminifera is presented as the number of individuals per gram of dry sediment [ind. g^{-1}] and
8 flux [ind. $\text{cm}^{-2} \text{y}^{-1}$]. Foraminifera species were grouped according to their ecological
9 tolerances. Four groups of indicators were distinguished: AW/frontal zone indicators, ArW
10 indicators, bottom current indicators and glaciomarine species (Majewski et al., 2009).
11 Morphologically similar species *Islandiella norcrossi* and *Islandiella helenae* are reported as
12 *Islandiella* spp.

14 **3.5 Stable isotopes analysis**

15 Carbon and oxygen stable isotope analyses were performed on *C. lobatulus* tests
16 selected from 27 sediment layers. From 10 to 12 specimens were collected from each sample
17 and subjected to ultrasonic cleaning. The measurements were performed on a Finningan MAT
18 253 mass spectrometer coupled to a Kiel IV carbonate preparation device at the University of
19 Florida. The resulting values are expressed in standard δ notation relative to Vienna Pee Dee
20 Belemnite (VPDB).

22 **3.6 Ancient DNA analysis**

23 Total DNA was extracted from approximately 10 g sediment using a Power Max Soil
24 DNA extraction kit (MoBio). The foraminiferal SSU rDNA fragment containing the 37f
25 hypervariable region was PCR amplified using primers tagged with unique sequences of five
26 nucleotides appended to their 5' ends (denoted by Xs), namely the foraminifera-specific
27 forward primer s14F1 (5'-XXXXXXCGGACACACTGAGGATTGACAG-3') and the reverse
28 primer s15 (5'-XXXXXCCTATCACATAATCATGAAAG-3'). The diatom DNA fragment
29 located in the V4 region was amplified with the forward DIV4for (5'-
30 XXXXXXXXGCGGTAATCCAGCTCCAATAG-3') and reverse DIV4rev3 (5'-
31 XXXXXXXXCTCTGACAATGGAATACGAATA-3') primers tagged with a unique
32 combination of eight nucleotides (denoted by Xs) attached at each primer's 5'-extremity. The
33 amplicons were purified using the High Pure PCR Cleanup Micro Kit (Roche) and quantified
34 using a Qubit 2.0 fluorometer. Samples were pooled in equimolar quantities and the sequence



1 library was prepared using a TruSeq library-preparation kit (Illumina). Samples were then
2 loaded into a MiSeq instrument for a paired-end run of 2*150 cycles (foraminifera) and 2*250
3 cycles (diatoms). The processing of the HTS sequence data including quality filtering, sample
4 demultiplexing, strict dereplication into unique sequences and operational taxonomic units
5 (OTU) selection was performed according to procedures described by Lejzerowicz et al.
6 (2013) and Pawłowska et al. (2014). The results are presented in OTU-to-sample tables and
7 transformed in terms of the number of sequences, number of OTUs and the percentage (%) of
8 sequences.

9

10 **4. Results**

11

12 **4.1 Sediment age and type**

13 All dates were in the chronological order and the uppermost layer contained modern,
14 post-bomb carbon indicating a post-1960 age (Table 1). Samples from depths of 2.5 cm and
15 5.5 cm were not calibrated because they revealed ages that were invalid for the selected
16 calibration curve. The age model was therefore based on the three remaining dates using a
17 linear interpolation. The age of the bottom of the core was estimated to be approximately 9 cal
18 ka BP (Fig. 2). However, the extremely low time resolution between 9 cal ka BP and 4 cal ka
19 BP precluded making any general conclusion about that interval. Therefore, the manuscript
20 focuses only on the last 4 cal ka BP (the Neoglacial).

21 The sediment accumulation rate (SAR) prior to ~ 2.7 cal ka BP was 0.002 cm y⁻¹. The
22 approximately 10-fold increase in SAR is noted at ~ 2.7 cal ka BP, when it increased to 0.023
23 cm y⁻¹. During the last 1.5 cal ka BP, SAR decreased to 0.01 cm y⁻¹ (Fig. 3). The amount of
24 IRD was the highest prior to ~ 2.7 cal ka BP, reaching up to 83 grains g⁻¹. After 2.7 cal ka BP,
25 the amount of IRD was relatively stable and did not exceed 18 grains g⁻¹. The flux of IRD
26 slightly decreased with time to 0.37 grains g⁻¹ cm⁻¹, except for one peak ~ 2.6 cal ka BP, when
27 it reached 0.8 grains g⁻¹ cm⁻¹ (Fig. 3).

28 The mean grain size of the 0-63-µm fraction had its highest value (5.8 φ) at ~ 2.7 cal
29 ka BP (Fig. 3) and after 2.4 cal ka BP a slight but continuous reduction in the mean 0-63-µm
30 grain size was noted. The minimum grain size (6.23 φ) was recorded at the top of the core.

31

32 **4.2 Stable isotopes**

33 The δ¹⁸O values were relatively stable prior to ~ 2.7 cal ka BP, varying slightly
34 between 3.55‰ and 3.69‰ vs. VPDB. Between ~ 2.7 and 1.5 cal ka BP, δ¹⁸O showed the



1 strongest variation, with values ranging from 3.28‰ to 3.77‰ vs. VPDB. After ~ 1.5 cal ka
2 BP, $\delta^{18}\text{O}$ became slightly lighter and varied between 3.43‰ and 3.64‰ vs. VPDB except for
3 one peak noted in the uppermost layer of the core, where $\delta^{18}\text{O}$ reached 3.87‰ vs. VPDB (Fig.
4 3). $\delta^{13}\text{C}$ values varied throughout the core with slightly lighter values, ranging from 0.92‰ to
5 1.12‰ vs. VPDB prior to ~ 2.7 cal ka BP. $\delta^{13}\text{C}$ values reaching up to 1.46‰ vs. VPDB were
6 noted between ~ 2.7 and ~ 1.5 cal ka BP and gradually decreased from ~ 1.5 cal ka BP to the
7 present, reaching 0.81‰ vs. VPDB at the top of the core (Fig. 3).

8

9 4.3 Fossil foraminifera

10 A total of 8647 fossil foraminifera specimens belonging to 47 species were identified
11 (Supplementary Fig. 1). The foraminiferal assemblages were dominated by calcareous taxa
12 which account for 62–98% of the foraminifera specimens except in the uppermost layer of the
13 core, where the percentage of calcareous foraminifera decreased to 44% (Fig. 3). There were
14 few peaks of agglutinated foraminifera noted at 2.0 cal ka BP, 1.8 cal ka BP and on the
15 sediment surface, where the percentages reached 37%, 37% and 66%, respectively (Fig. 3).
16 The number of foraminiferal individuals varied from 156 to 2610 ind. g^{-1} and the lowest
17 abundances were observed prior to ~ 2.7 cal ka BP (Fig. 3). A short-term decrease in the
18 foraminiferal abundance was observed between 2.1 and 1.9 ka BP, with values reaching as
19 low as 304 ind. g^{-1} . The abundance maxima were noted at 2.3, 1.5, and 0.6 ka BP, with values
20 reaching 2524 ind. g^{-1} , 2584 ind. g^{-1} , and 2610 ind. g^{-1} , respectively. The foraminiferal flux
21 was low and relatively stable throughout the core with values that did not exceed 1 ind $\text{cm}^{-2} \text{y}^{-1}$
22 ¹, except for two peaks at 2.3 and 1.5 ka BP, when the flux reached 2.2 ind $\text{cm}^{-2} \text{y}^{-1}$ (Fig. 3).

23 The abundances of certain species followed a general trend with maxima ~ 2.3 cal ka
24 BP and after ~ 1.7 cal ka BP and minima prior to ~ 2.7 cal ka BP and between 2.3 and 1.7 cal
25 ka BP. The most abundant species was *Cassidulina reniforme*, with densities reaching up to
26 900 ind g^{-1} . The other species that constituted the majority of the foraminiferal assemblage
27 were *Buccella frigida*, *Cibicides lobatulus*, *Elphidium excavatum*, *Islandiella* spp, *Melonis*
28 *barleeianum*, and *Nonionellina labradorica* (Fig. 4).

29 The foraminiferal assemblage prior to ~ 2.7 cal ka BP was codominated by
30 *Nonionellina labradorica* and *Melonis barleeianum*, which are species that are considered to
31 be indicators of AW inflow and/or frontal zones, and glaciomarine taxa, primarily
32 *Cassidulina reniforme* and *Elphidium excavatum*, which together accounted for up to 60% of
33 the foraminiferal abundance (Fig. 4). After ~ 2.7 cal ka BP, there were AW/frontal zone
34 indicator peaks recorded at 2.4 and 1.8 cal ka BP, where the percentages increased to 33%,



1 28%, and 42% of the total abundance. The period between ~ 2.4 cal ka BP and ~ 1.8 cal ka
2 BP was characterized by an increase in the percentage of sea-ice indicators (*B. frigida* and
3 *Islandiella* spp), which accounted for up to 25% of the total abundance, and by a short-term
4 peak in the glaciomarine taxa, which accounted for up to 49% of foraminiferal assemblage
5 between 2.5 and 2.1 cal ka BP. A decrease in the relative abundance of glaciomarine species
6 was observed after ~ 0.5 cal ka BP and was followed by an increase in the AW/frontal zone
7 indicators and a single peak in the percentage of bottom current indicators, which reached
8 19% (Fig. 4).

9

10 **4.4 Foraminiferal aDNA sequences**

11 A total of 1,499,889 foraminiferal DNA sequences were clustered into 263 OTUs, and
12 20 remained unassigned. The remaining OTUs were assigned to Globigerinida (5 OTUs),
13 Robertinida (1 OTU), Rotaliida (49 OTUs), Textulariida (18 OTUs), Monothalamea (163
14 OTUs), and Miliolida (7 OTUs). The majority of sequences belonged to Monothalamea
15 (60%) and Rotaliida (31%) (Supplementary Fig. 2). Herein, we focus on Monothalamea,
16 which is the dominant component of the foraminiferal aDNA record.

17 The most important components of the monothalamous assemblage were *Micrometula*
18 sp., *Cylindrogullmia* sp., *Hippocrepinella hirudinea*, *Ovammia* sp., *Nemogullmia* sp.,
19 *Tinogullmia* sp., *Cedhagenia saltatus*, undetermined allogromiids belonging to clades A and
20 Y (herein called “allogromiids”), and sequences belonging to taxa known exclusively from
21 environmental sequencing (herein called “environmental clades”). The sequences belonging
22 to allogromiids were present throughout the core, accounting for 16–31.7% of all the
23 foraminiferal sequences, except during the intervals prior to ~ 2.4 cal ka BP and ~ 1.7 cal ka
24 BP, when contribution of allogromiid sequences decreased to less than 10% (Fig. 5). The
25 majority of the allogromiids belonged to clade Y, which accounted for up to 100% of the
26 allogromiid sequences, except for the two peaks at 1.6–1.7 cal ka BP and 2.4–2.6 cal ka BP,
27 when the majority of allogromiid sequences belonged to clade A (Fig. 6).

28 The periods prior to ~ 2.4 cal ka BP and ~ 1.7 cal ka BP were marked by the
29 disappearance of sequences belonging to *C. saltatus*, *Nemogullmia* sp., and the environmental
30 clades, followed by an increase in the percentages of sequences belonging to *Micrometula* sp.,
31 *Ovammia* sp., *Tinogullmia* sp., *Shepherdella* sp. and *Cylindrogullmia* sp. (Fig. 5).

32

33 **4.5 Diatom aDNA sequences**



1 A total of 824,546 diatom DNA sequences were clustered into 177 OTUs.
2 considerable part of the diatom sequences was assigned to only higher taxonomic levels (i.e.
3 Mediophyceae; 34% of diatom sequences) or to raphid pennate forms (13% of diatom
4 sequences; Supplementary Fig. 3). The most abundantly sequenced diatom taxa were
5 *Thalassiosira* spp, *Navicula* sp. and *Chaetoceros* sp. *Navicula* sp. was the most abundant ~3.3
6 cal ka BP, accounting for up to 25.5% of all diatom sequences. In the following periods,
7 *Navicula* sp. also occurred at ~ 2.6 cal ka BP, ~ 1.7 cal ka BP, ~ 1.3 cal ka BP, and ~ 0.9 cal
8 ka BP, but its abundance did not exceed 5% (Fig. 7). The percentage of sequences of
9 *Chaetoceros* sp. decreased downcore, from 78% at the surface to 3% at ~ 2.2 cal ka BP (Fig.
10 7). The sequences of *Thalassiosira* spp. were most abundant between ~ 2.6 cal ka BP and ~
11 0.9 cal ka BP, accounting for up to 61% of all diatom sequences. The majority of these
12 sequences were assigned to *Thalassiosira* sp., the remaining sequences belonged to
13 *Thalassiosira antarctica* and *Thalassiosira hispida*. Both *Thalassiosira* sp. and *T. antarctica*
14 were detected throughout the core and the percentages of their sequences were the highest
15 prior to ~ 0.9 cal ka BP, reaching up to 50% and 19%, respectively (Fig. 7). Sequences of *T.*
16 *hispida* were noted only at the sediment core surface, and ~ 2.2 cal ka BP, ~ 1.7 cal ka BP,
17 and ~ 1.6 cal ka BP, accounting for up to 5%, 0.7%, 1.2%, and 0.1% of the diatom sequences
18 (Fig. 7).

19

20 6. Discussion

21 The ST_{1.5} age model is based on the linear interpolation between the three dates, so
22 the age control of the core should be treated with caution, however the timing of the major
23 environmental shifts was well supported by the variation in ST_{1.5} grain size, the abundance
24 of fossil foraminifera and isotope composition of foraminiferal tests and molecular records of
25 diatoms and non-fossilized foraminifera. Moreover, the good correlation with other records
26 from the region (e.g., Sarnthein et al., 2003, Rasmussen and Thomsen, 2014) supports the
27 ST_{1.5} age model. The multiproxy record from Storfjorden revealed several intervals of
28 pronounced environmental changes. The major environmental shifts occurred at ~ 2.7, 2.3 and
29 1.7 cal ka BP, what correlated well with the temperature minimum (2.7 cal ka BP) and
30 maxima (2.3 and 1.7 cal ka BP) recorded in the GISP2 core (Cuffey and Clow, 1997; Alley,
31 2000) and 23258 core (Sarnthein et al., 2003).

32 The most pronounced environmental change during the Neoglacial was recorded in
33 Storfjorden ~ 2.7 cal ka BP. During the period prior to ~ 2.7 cal ka BP, the ST_{1.5}
34 sedimentary record displayed elevated and variable IRD delivery and coarsening of the 0-63-



1 μm fraction (Fig. 3). These results are in agreement with the record from Storfjordrenna
2 (Łącka et al., 2015), where peaks in IRD were noted during the Neoglacial and were
3 attributed to increased iceberg rafting due to fluctuations in the glacial fronts (e.g. Forwick et
4 al., 2010). In addition, the relatively high mean grain size of the 0-63- μm fraction (Fig. 3)
5 might have resulted from more vigorous bottom currents and the removal of fine-grained
6 sediment. According to Andruleit et al. (1996) a sudden increase in the hydrodynamic energy
7 occurred during the late Holocene (~ 2.6 cal ka BP) at the SW Spitsbergen shelf. There are
8 multiple explanations for such an intensification of bottom currents activity, including
9 postglacial reorganization of the oceanographic conditions and a southward shift of the Polar
10 Front, relative isostatic lowering of the sea level, or outflows of dense BSW (Andruleit et al.,
11 1996). In Storfjorden, the intensification of bottom currents is most likely related to the
12 presence of coastal polynyas and BSW production (Haarpainter et al., 2001). The most
13 intensive brine production occurred in Storfjorden during the cold climatic intervals and was
14 associated with the presence of extensive sea-ice cover (Rasmussen and Thomsen, 2015).

15 The ST_1.5 foraminiferal record supports the presence of a sea-ice cover in
16 Storfjorden during the first phase of the Neoglacial (prior to ~ 2.7 cal ka BP). The ST_1.5
17 foraminiferal assemblage was codominated by glacier-proximal fauna (primarily *C.*
18 *reniforme*) and indicators of frontal zones (primarily *M. barleeaanum*; Fig. 4). The presence of
19 *C. reniforme* and *M. barleeaanus* is linked to cooled and salty AW (e.g., Hald and Steinsund,
20 1996; Jernas et al., 2013). Moreover, these species are also associated with the presence of
21 phytodetritus, which may be related to the high productivity observed in frontal zones and/or
22 near the sea-ice edge (Jennings et al., 2004). Knies et al. (2017) suggested a variable sea-ice
23 cover extent and a fluctuating sea-ice margin in Storfjorden prior to ~ 2.8 cal ka BP. The
24 record of diatom aDNA supports the latter assumption because the dominant components of
25 the diatom assemblages were *Navicula* sp. and *Thalassiosira* spp (Fig. 7), which are genera
26 found within or under sea-ice (Cremer, 1999; Ikävalko, 2004). The presence of these diatom
27 taxa may suggest that primary production at that time was primarily associated with the
28 winter–spring formation of the sea-ice cover.

29 The typical response of a foraminiferal community to high trophic resources is an
30 increase in diversity and standing stock (Wollenburg and Kuhnt, 2000). However, according
31 to our data, the foraminiferal community showed no clear signs of increased productivity, as
32 the abundance and flux of foraminifera were low prior to ~ 2.7 cal ka BP (Fig. 3). Similarly,
33 Rasmussen and Thomsen (2015) noted a decrease in concentration of benthic foraminifera in
34 Storfjorden at that time, which was attributed to the more extensive seasonal sea-ice cover.



1 The lack of a growth response in the benthic foraminifera communities to an increased food
2 supply was also observed in the costal polynyas off Greenland (Ahrens et al., 1997).
3 Conversely, Smith et al. (2010) attributed higher abundances of planktonic and benthic
4 foraminifera in the Weddell Sea coastal polynya to organic matter deposition in the seasonally
5 open-marine environment. The periodic melting and freezing of Storfjorden polynya may
6 enhance the primary productivity; however, at the same time production of dense brines may
7 limit the growth and reproduction of foraminifera. This latter assumption needs to be
8 confirmed by further studies.

9 The environmental conditions in central Storfjorden changed noticeably ~ 2.7 cal ka
10 BP. The increase in SAR was followed by a gradual decrease in the 0-63- μ m fraction and a
11 decrease in the IRD delivery after ~ 2.7 cal ka BP (Fig. 3). According to Knies et al. (2017),
12 the distinct surface water cooling during the Neoglacial provides a prerequisite for the
13 presence of more extensive sea-ice cover; therefore inner Storfjorden was covered by densely
14 packed sea ice between ~ 2.8 and 0.5 cal ka BP with low entrainment of terrestrial sediment
15 and diminished surface water productivity. Rasmussen and Thomsen (2015) suggested glacial
16 advance, followed by intensive ice rafting and meltwater delivery at that time. Therefore, the
17 decreasing IRD in the ST_1.5 core may result from the presence of a sea-ice cover that
18 reduced iceberg rafting while the majority of coarse grained material settled in the proximity
19 of the glacial fronts. Similar conclusions have been stated by Forwick and Vorren (2009) and
20 Forwick et al. (2010), who assumed that the enhanced formation of sea ice along the West
21 Spitsbergen coast trapped icebergs inside the Isfjorden system. Furthermore, glaciers supply
22 the fjord with large amounts of turbid meltwater, leading to the intensive settling of sediment
23 and an increase in sediment accumulation (Fig. 3). The accumulation of fine sediment may
24 also be enhanced by the slowdown of the bottom currents, indicated by the decrease in the 0-
25 63- μ m fraction after ~ 2.7 cal ka BP (Fig. 3).

26 Both heavy ice cover and meltwater delivery may limit light penetration in the water
27 and therefore suppress primary production and organic matter export to the bottom. However,
28 the foraminiferal fauna in central Storfjorden revealed more than a 10-fold increase in flux
29 and abundance followed by short-term fluctuations after ~ 2.7 cal ka BP (Fig. 3); this may
30 suggest favorable conditions for foraminiferal growth. Paleoceanographic records from the
31 Nordic Seas suggest that the Neoglacial was not a constantly cold period. For example, the
32 western Spitsbergen continental margin experienced periods of a rapidly advancing and
33 retreating sea-ice margin, caused by a temporarily strengthened AW inflow and/or changes in
34 the atmospheric circulation patterns (Müller et al., 2012). Sarnthein et al. (2003) reported two



1 intervals of remarkably warmer sea surface on the western continental margin of the Barents
2 Sea at ~ 2.2 and ~ 1.7 cal ka BP, which was attributed to short-term pulses of warm AW
3 advection. The ST_1.5 micropaleontological and molecular records are in agreement with the
4 findings of Sarnthein et al. (2003). The inflows of AW ~ 2.3 cal ka BP and 1.7 cal ka BP were
5 marked by peaks in the total foraminiferal abundance in general (Fig. 3) and peaks in the
6 percentage of AW foraminiferal indicators, in particular (Fig. 4), followed by the occurrence
7 of sequences of *T. hispida* (Fig. 7), a diatom species characteristic of subpolar and temperate
8 regions (Katsuki et al., 2009).

9 Knies et al. (2017) have suggested that the pulses of advected AW did not influence
10 the persistent sea-ice cover in Storfjorden between ~ 2.8 and 0.5 cal ka BP. However, the
11 ST_1.5 foraminiferal record indicates that central Storfjorden was not constantly covered by
12 sea ice at that time. A more reasonable scenario is surface water cooling and periodic melting
13 and freezing of the sea surface and consequent production of brines, which launched
14 convective water mixing and nutrient resupply to the surface, thereby stimulating primary
15 production (Łącka et al., *in prep.*). The presence of diatom aDNA sequences throughout the
16 Neoglacial (Fig. 7) may suggest continuous primary production. It is likely that pulses of AW
17 inflow at 2.3 cal ka BP and 1.7 cal ka BP induced melting of the ice cover, leading to the
18 formation of ice-free areas and highly productive ice marginal zones. This conjecture may be
19 supported by peaks in the light $\delta^{18}\text{O}$ in benthic foraminiferal tests, the maxima of the
20 foraminiferal flux (Fig. 3) and peaks in the abundance of species associated with highly
21 productive environments such as *M. barleeanum* and *N. labradorica* (Fig. 4). Similarly, the
22 foraminiferal flux and abundance were elevated and slightly variable after ~ 1.7 cal ka BP.
23 The foraminiferal assemblage was codominated by AW/frontal zone indicators and
24 glaciomarine species (Fig. 4) at that time, which may suggest rather ameliorated
25 environmental conditions. In contrast, the interval between 2.3 and 1.7 cal ka BP featured
26 slightly heavier $\delta^{13}\text{C}$ and $\delta^{18}\text{O}$ followed by a decrease in the foraminiferal flux and abundance
27 (Fig. 3). The foraminiferal assemblage at this time was dominated by glaciomarine and sea-
28 ice taxa (Fig. 4), which indicate more severe environmental conditions with extensive ice
29 cover and suppressed productivity. The sea-ice formation led to a more intensive release of
30 brines and consequently, stronger bottom current activity reflected in a slight increase in the
31 percentage of *C. lobatulus*, which is considered to be a bottom current indicator (Fig. 4).

32 The above-described environmental changes were also reflected in the aDNA record
33 of monothalamous foraminifera. During the time intervals of 2.2–1.9 cal ka BP and 1.3–0.4
34 cal ka BP, monothalamous foraminifera was dominated by allogromiids belonging to clade Y,



1 *Nemogullmia* sp., *C. saltatus* and monothalamids belonging to so called “environmental
2 clades” (Fig. 5). Allogromiids are not coherent taxonomic group but are scattered between
3 several monothalamous clades (Gooday 2002; Pawłowski et al., 2002). Considerable part of
4 the allogromiid sequences in the ST_1.5 core belong to clade Y (Fig. 6), which is primarily
5 composed of taxa known only from environmental sequencing. Sequences belonging to clade
6 Y have previously been noted in modern sediments in the Spitsbergen fjords (Pawłowska et
7 al., *in prep.*). Moreover, clade Y has been abundantly sequenced in the coastal areas off
8 Scotland, characterized by high levels of environmental disturbances (Pawłowski et al.,
9 2014a); this might suggest its high tolerance to environmental stress. In addition, so called
10 “environmental clades” comprised of monothalamous taxa known exclusively from
11 environmental sequencing (Lecroq et al., 2011) and may belong to novel, undescribed
12 foraminiferal lineages (Pawłowski et al., 2014b). *C. saltatus* was recently found by Gooday et
13 al. (2011) in the Black Sea and until recently, little has been known about its environmental
14 tolerances; however, its occurrence in areas with high levels of pollution suggests that it is an
15 opportunistic species with a high tolerance to environmental disturbances. Specimens of
16 *Nemogullmia* were also found in the Spitsbergen fjords (Gooday et al., 2005; Majewski et al.,
17 2005); however, data on its abundance and distribution may be incomplete due to the
18 degradation of its fragile, organic-walled tests. The abovementioned taxa nearly disappeared
19 during episodes of enhanced AW inflow ~ 2.4 cal ka BP and ~ 1.7 cal ka BP, and the
20 monothalamous assemblage was dominated at that time by *Micrometula* sp., *Ovammina* sp.,
21 *Shepherdella* sp., *Tinogullmia* sp., *Cylindrogullmia* sp., and allogromiids belonging to clade
22 A (Fig. 5; Fig. 6). All these taxa have recently been observed in the fjords of Svalbard (e.g.
23 Gooday et al., 2005; Majewski et al., 2005; Sabbattini et al., 2007; Pawłowska et al., 2014).
24 *Cylindrogullmia* sp. commonly been found in the inner parts of the fjords (Gooday et al.,
25 2005). Hughes and Gooday (2004) suggest that *Cylindrogullmia* sp. is an infaunal species that
26 normally resides in deeper sediment layers of sediment. *Micrometula* sp. was among the
27 abundantly found organic-walled allogromiids in glacier-proximal sites off Novaya Zemlya
28 (Korsun & Hald, 1998; Korsun et al., 2005) and Svalbard (Korsun & Hald, 2000; Gooday et
29 al., 2005; Pawłowska et al., 2014). Moreover, *Cylindrogullmia* and *Micrometula* are
30 dependent on the presence of fresh phytodetritus (Alve, 2010). *Ovammina* sp. feeds on
31 diatoms and other forms of microalgae (Goldstein & Alve, 2011). Similarly, the presence of
32 *Tinogullmia* is largely controlled by the presence of organic material on the seafloor. High
33 concentrations of *Tinogullmia* have been found in coastal (Cornelius & Gooday, 2004) and
34 deep-sea regions (Gooday, 1993) within phytodetrital aggregates.



1 In general, monothalamous foraminifera are highly adaptable and resistant to
2 environmental disturbances. However, the taxa that dominated the monothalamous
3 assemblage during warm intervals seem to be responsive to the delivery of organic matter and
4 may flourish during phytoplankton blooms associated with the settling of organic matter (e.g.,
5 Alve, 2010; Sabbattini et al., 2012, 2013). The pulses of AW inflow that are associated with
6 sea-ice melting stimulated phytoplankton blooms and organic matter supply to the bottom.
7 The enhanced primary productivity supported the development of an organic matter-
8 dependent monothalamous community. Conversely, the colder phases of the Neoglacial were
9 characterized by heavy and densely packed sea ice resulting in limited productivity (Knies et
10 al., 2017). Therefore, the monothalamous assemblage was less diverse and was dominated by
11 highly opportunistic taxa.

12 The decrease in the percentage of foraminiferal sea-ice indicators that started after ~
13 1.7 cal ka BP suggests a gradually diminishing sea-ice coverage in Storfjorden (Fig. 4), and
14 Modern-like conditions were established in Storfjorden ~ 0.5 cal ka BP, with seasonally
15 variable sea-ice cover resulting in intensified but variable polynyal activity (Rasmussen and
16 Thomsen, 2014; Knies et al., 2017). the IP₂₅ records from the western Spitsbergen shelf
17 indicate variable sea-ice conditions during the last 2 ka (Cabedo-Sanz and Belt, 2016).
18 Moreover, the majority of diatom aDNA sequences after ~ 0.5 cal ka BP belonged to
19 *Chaetoceros* sp., a taxa that is observed in surface waters and is almost entirely absent under
20 sea ice (Róžańska et al., 2008). Moreover, high abundances of *Chaetoceros* are often
21 associated with highly productive surface waters (Cremer, 1999), which indicate declining
22 sea-ice cover (Cabedo-Sanz and Belt, 2016). However, the aDNA record of the
23 monothalamous foraminifera ~ 0.4 cal ka BP displayed relatively high percentages of taxa
24 that dominated during colder intervals of the Neoglacial (Fig. 5); this may be related to the
25 recovery from the Little Ice Age and consequently, temporarily deteriorated environmental
26 conditions (D'Andrea et al., 2012). However, further studies are required to confirm the latter
27 conclusion.

28

29 7. Conclusions

30 The ST_1.5 multiproxy record revealed that the environmental variability in Storfjorden
31 during the Neoglacial was steered controlled primarily by the interplay between AW and ArW
32 and changes in the sea-ice cover. The molecular record supports and complements
33 sedimentary and microfossil records, which indicate that major changes in the environmental
34 conditions in Storfjorden occurred at ~ 2.7 cal ka BP. The general cooling at the early phase



1 of the Neoglacial initiated conditions for the formation of extensive sea-ice cover. The latter
2 part of the Neoglacial (after ~ 2.7 cal ka BP) was characterized by alternating short-term
3 cooling and warming periods. Warming was associated with pulsed inflows of AW and sea-
4 ice melting stimulating phytoplankton blooms and organic matter supply to the bottom. The
5 cold phases were characterized by heavy and densely packed sea ice resulting in limited
6 productivity.

7 Moreover, the aDNA diatom record supports the conclusion that primary production took
8 place continuously during the Neoglacial, regardless of the sea-ice conditions. The early
9 phase of the Neoglacial was characterized by the presence of diatom taxa associated with sea
10 ice, whereas the present-day diatom assemblage was dominated by *Chaetoceros* spp, a taxa
11 characteristic of open water.

12 The aDNA record of monothalamous foraminifera is in agreement with the microfossil
13 record and revealed the timing of the major pulses of AW at 2.3 and 1.7 cal ka BP. The AW
14 inflow was marked by an increase in the percentage of sequences of monothalamous taxa
15 associated with the presence of fresh phytodetritus. The monothalamous assemblage during
16 cold intervals was less diverse and was dominated by monothalamous foraminifera known
17 only from environmental sequencing.

18

19 **Author contribution**

20 MZ and Jan P designed the study. Joanna P, MŁ and MZ collected the sediment core. MŁ and
21 MK performed the sedimentological and micropaleontological analyses. Joanna P performed
22 the molecular analyses and prepared the manuscript with contributions from all co-authors.

23

24 **Acknowledgements**

25 The study was supported by the National Science Centre grants no. 2015/19/D/ST10/00244
26 and 2016/21/B/ST10/02308, and Swiss National Science Foundation grant no.
27 31003A_179125.

28

29 **References**

30 Ahrens, M.J., Graf, G., Altenbach, A.V.: Spatial and temporal distribution patterns of benthic
31 foraminifera in the Northeast Water Polynya, Greenland. *J. Marine Syst.* 10, 445-465,
32 [https://doi.org/10.1016/S0924-7963\(96\)00052-8](https://doi.org/10.1016/S0924-7963(96)00052-8), 1997.



- 1 Alve, E.: Benthic foraminiferal responses to absence of fresh phytodetritus: A two – year
2 experiment, *Mar. Micropaleontol.*, 76, 67-76, <https://doi.org/10.1016/j.marmicro.2010.05.003>,
3 2010.
- 4 Andersen, C., Koç, N., Moros, M.: A highly unstable Holocene climate in the subpolar North
5 Atlantic: evidence from diatoms, *Quat. Sci. Rev.*, 23, 2155-2166,
6 <https://doi.org/10.1016/j.quascirev.2004.08.004>, 2004.
- 7 Andruleit, H., Freiwald, A., Schäfer, P.: Bioclastic carbonate sediments on the southwestern
8 Svalbard shelf, *Mar. Geol.* 134, 163-182, [https://doi.org/10.1016/0025-3227\(96\)00044-8](https://doi.org/10.1016/0025-3227(96)00044-8),
9 1996.
- 10 Årthun, M., Ingvaldsen, R.B., Smedsrud, L.H., Schrum, C.: Dense water formation and
11 circulation in the Barents Sea, *Deep Sea Res. Part I: Oceanogr. Res. Pap.*, 58, 801-817,
12 <https://doi.org/10.1016/j.dsr.2011.06.001>, 2011.
- 13 Berger, A.L.: Long-term variations of daily insolation and quaternary climatic changes, *J.*
14 *Atmos. Sci.*, 35, 2362-2367, [https://doi.org/10.1175/1520-0469\(1978\)035<2362:LTVODI>2.0.CO;2](https://doi.org/10.1175/1520-0469(1978)035<2362:LTVODI>2.0.CO;2) 1978.
- 16 Blott, S.J., Pye, K.: GRADISTAT: a grain size distribution and statistics package for the
17 analysis of unconsolidated sediments, *Earth Surf. Process. Landf.*, 26, 1237 – 1248,
18 <https://doi.org/10.1002/esp.261>, 2001.
- 19 Cabedo-Sanz, P., Belt, S.T.: Seasonal sea ice variability in eastern Fram Strait over the last
20 2000 years, *Arktos*, 2, 22, doi: 10.1007/s41063-016-0023-2, 2016.
- 21 Boere, A.C., Abbas, B., Rijpstra, W.I.C., Versteegh, G.J., Volkman, J.K., Sinninghe Damsté,
22 J.S., Coolen, M.J.L.: Late-Holocene succession of dinoflagellates in an Antarctic fjord using a
23 multi-proxy approach: paleoenvironmental genomics, lipid biomarkers and palynomorphs,
24 *Geobiol.*, 7, 265-281, <https://doi.org/10.1111/j.1472-4669.2009.00202.x>, 2009.
- 25 Calvo, E., Grimalt, J., Jansen, E.: High resolution U_{37}^K sea surface temperature reconstruction
26 in the Norwegian Sea during the Holocene. *Quat. Sci. Rev.*, 21, 1385-1394,
27 [https://doi.org/10.1016/S0277-3791\(01\)00096-8](https://doi.org/10.1016/S0277-3791(01)00096-8), 2002.
- 28 Cornelius, N., Gooday, A.J.: ‘Live’ (stained) deep-sea benthic foraminiferans in the western
29 Weddell Sea: trends in abundance, diversity and taxonomic composition along a depth
30 transect, *Deep Sea Res. II*, 51, 1571-1602, <https://doi.org/10.1016/j.dsr2.2004.06.024>, 2004.
- 31 Cremer, H.: Distribution patterns of diatom surface sediment assemblages in the Laptev Sea
32 (Arctic Ocean), *Mar. Micropaleontol.*, 38, 39-67, [https://doi.org/10.1016/S0377-8398\(99\)00037-7](https://doi.org/10.1016/S0377-8398(99)00037-7), 1999.



- 1 Cuffey, K.M., Clow, G.D.: Temperature, accumulation, and ice sheet elevation in central
2 Greenland through the last deglacial transition, *J. Geophys. Res.*, 102, 26383-26396
3 <https://doi.org/10.1029/96JC03981>, 1997.
- 4 D'Andrea, W.J., Vaillencourt, D.A., Balascio, N.L., Werner, A., Roof, S.R., Retelle, M.,
5 Bradley, R.S.: Mid Little Ice Age and unprecedented recent warmth in an 1800 year lake
6 sediment record from Svalbard, *Geology*, 40, 1007-1010, <https://doi.org/10.1130/G33365.1>,
7 2012.
- 8 Forwick, M., Vorren, T.O.: Late Weichselian and Holocene sedimentary environments and
9 ice rafting in Isfjorden, Spitsbergen, *Palaeogeogr. Palaeoclimatol. Palaeoecol.* 280, 258-274,
10 <https://doi.org/10.1016/j.palaeo.2009.06.026>, 2009.
- 11 Forwick, M., Vorren, T.O., Hald, M., Korsun, S., Roh, Y., Vogt, C., Yoo, K.-C.: Spatial and
12 temporal influence of glaciers and rivers on the sedimentary environment in Sassenfjorden
13 and Tempelfjorden, Spitsbergen. In: Geological Society, London, Special Publications, vol
14 344 (1): 163-193, <https://doi.org/10.1144/SP344.13>, 2010.
- 15 Geyer, F., Fer, I., Smedsrud, L. H.: Structure and forcing of the overflow at the Storfjorden
16 sill and its connection to the Arctic coastal polynya in Storfjorden, *Ocean Sci.*, 6(1), 401-411,
17 <https://doi.org/10.5194/os-6-401-2010>, 2010.
- 18 Goldstein, S.T., Alve, E.: Experimental assembly of foraminiferal communities from coastal
19 propagule banks, *Mar. Ecol. Prog. Ser.* 437, 1-11, <https://doi.org/10.3354/meps09296>,
20 2011.
- 21 Gooday, A.J.: Deep-sea benthic foraminiferal species which exploit phytodetritus:
22 Characteristic features and controls on distribution, *Mar. Micropaleontol.*, 22, 187-205,
23 [https://doi.org/10.1016/0377-8398\(93\)90043-W](https://doi.org/10.1016/0377-8398(93)90043-W), 1993.
- 24 Gooday, A.J.: Organic-walled allogromiids: aspects of their occurrence, diversity and ecology
25 in marine habitats, *J. Foramin. Res.*, 32, 384-399, <https://doi.org/10.2113/0320384>, 2002.
- 26 Gooday, A.J., Bowser, S.S., Cedhagen, T., Cornelius, N., Hald, M., Korsun, S., Pawłowski,
27 J.: Monothalamous foraminiferans and gromiids (Protista) from western Svalbard: A
28 preliminary survey, *Mar. Biol. Res.*, 1, 290 – 312,
29 <https://doi.org/10.1080/17451000510019150>, 2005.
- 30 Gooday, A.J., Anikeeva, O.V., Pawłowski, J.: New genera and species of monothalamous
31 Foraminifera from Bataclava and Kazach'ya Bays (Crimean Peninsula, Black Sea), *Mar.*
32 *Biodiv.*, 41, 481-494, <https://doi.org/10.1007/s12526-010-0075-7>, 2011.



- 1 Haarpainter, J., Gascard, J.C., Haugan, P.M.: Ice production and brine formation in
2 Storfjorden, Svalbard, *J. Geophys. Res.* *106* C7, 14 001–14 013,
3 <https://doi.org/10.1029/1999JC000133>, 2001.
- 4 Hald, M. Steinsund, P.I.: Benthic foraminifera and carbonate dissolution in the
5 surface sediments of the Barents and Kara Seas, *Berichte zur Polarforschung*, 212,
6 285–307, 1996.
- 7 Hansen, J., Hanken, N.-M., Nielsen, J.K., Nielsen, J.K., Thomsen, E.: Late Pleistocene and
8 Holocene distribution of *Mytilus edulis* in the Barents Sea region and its paleoclimatic
9 implications, *J. Biogeogr.* 38, 1197–1212, <https://doi.org/10.1111/j.1365-2699.2010.02473.x>,
10 2011.
- 11 Hughes, J.A., Gooday, A.J.: Associations between living benthic foraminifera and dead tests
12 of *Syringammina fragilissima* (Xenophyophorea) in the Darwin Mounds region (NE Atlantic),
13 *Deep Sea Res. Part I: Oceanographic Research Papers*, 51, 1741–1758,
14 <https://doi.org/10.1016/j.dsr.2004.06.004>, 2004.
- 15 Ikävalko, J.: Checklist of unicellular and invertebrate organisms within and closely associated
16 with sea ice in the Arctic regions. MERI – Report Series of the Finnish Institute of Marine
17 Research, 52, Helsinki, Finland, Finnish Institute of Marine Research, 2004.
- 18 Jennings, A.E., Weiner, N.J., Helgadottir, G., Andrews, J.T.: Modern foraminiferal faunas of
19 the southwestern to northern Iceland Shelf; oceanographic and environmental controls, *J.*
20 *Foramin. Res.*, 34, 180–207, <https://doi.org/10.2113/34.3.180>, 2004.
- 21 Jernas, P., Klitgaard Kristensen, D., Husum, K., Wilson, L., Koç, N.: Palaeoenvironmental
22 changes of the last two millennia on the western and northern Svalbard shelf, *Boreas*, 42, 236–
23 255, <https://doi.org/10.1111/j.1502-3885.2012.00293.x>, 2013.
- 24 Katsuki, K., Takahashi, K., Onodera, J., Jordan, R.W., Suto, I.: Living diatoms in the vicinity
25 of the North Pole, summer 2004, *Micropaleontol.* 55, 137–170, 2009.
- 26 Killworth, P.D.: Deep convection in the World Ocean, *Rev. Geophys.*, 21, 1–26,
27 [doi:10.1029/RG021i001p00001](https://doi.org/10.1029/RG021i001p00001), 1983.
- 28 Knies, J., Pathirana, I., Cabedo-sanz, P., Banica, A., Fabian, K., Rasmussen, T.L., Forwick,
29 M., Belt, S.: Sea-ice dynamics in an Arctic coastal polynya during the past 6500 years,
30 *Arktos*, 3, 1, <https://doi.org/10.1007/s41063-016-0027-y>, 2017.
- 31 Korsun, S., Hald, M.: Modern benthic Foraminifera off Novaya Zemlya tidewater glaciers,
32 *Arctic and Alpine Research*, 30, 61–77, <https://doi.org/10.1080/00040851.1998.12002876>,
33 1998.



- 1 Korsun, S., Hald, M.: Seasonal dynamics of benthic foraminifera in a glacially fed fjord of
2 Svalbard, European Arctic, *J. Foramin. Res.*, 30, 251-271, <https://doi.org/10.2113/0300251>,
3 2000.
- 4 Korsun, S., Pogodina, I.A., Forman, S.L., Lubinski, D.J.: Recent foraminifera in glaciomarine
5 sediments from three arctic fjords of Novaja Zemlja and Svalbard, *Polar Res.*, 14, 15 – 31,
6 <https://doi.org/10.1111/j.1751-8369.1995.tb00707.x>, 1995.
- 7 Lejzerowicz, F., Esling, P., Majewski, W., Szczuciński, W., Decelle, J., Obadia, C., Martinez
8 Arbizu, P., Pawłowski, J.: Ancient DNA complements microfossil record in deep-sea
9 subsurface sediments. *Biol. Lett.*, 9, 20130283, <https://doi.org/10.1098/rsbl.2013.0283>, 2013.
- 10 Lecroq B., Lejzerowicz F., Bachar D., Christen R., Esling P., Baerlocher L., Østerås M.,
11 Frinelli L., Pawłowski J.: Ultra-deep sequencing of foraminiferal microbarcodes unveils
12 hidden richness in deep-sea sediments, *PNAS*, 108:13177-82,
13 <https://doi.org/10.1073/pnas.1018426108>, 2011.
- 14 Lydersen, C., Nøst, O., Lovell, P., McConell, B., Gammelsrød, T., Hunter, C., Fedak, M.,
15 Kovacs, K.: Salinity and temperature structure of a freezing Arctic fjord – monitored by white
16 whales (*Delphinapterus leucas*), *Geophys. Res. Lett.*, 29, 2119,
17 <https://doi.org/10.1029/2002GL015462>, 2002.
- 18 Łacka, M., Zajączkowski, M., Forwick, M., Szczuciński, W.: Late Weichselian and Holocene
19 palaeoceanography of Storfjordrenna, southern Svalbard, *Clim. Past*, 11, 587-603,
20 <https://doi.org/10.5194/cp-11-587-2015>, 2015.
- 21 Majewski, W., Pawłowski, J., Zajączkowski, M. 2005. Monothalamous foraminifera from
22 West Spitsbergen fjords: a brief overview, *Polish Polar Res.*, 26(4), 269-285.
- 23 Majewski, W., Szczuciński, W., Zajączkowski, M.: Interactions of Arctic and Atlantic water-
24 masses and associated environmental changes during the last millennium, Hornsund (SW
25 Svalbard). *Boreas*, 38, 529-544, <https://doi.org/10.1111/j.1502-3885.2009.00091.x>, 2009.
- 26 Mangerud, J., Bondevik, S., Gulliksen, S., Hufthammer, A.K., Høseter, T.: Marine ¹⁴C
27 reservoir ages for 19th century whales and mollusks from the North Atlantic, *Quat. Sci. Rev.*,
28 25, 3228-3245, <https://doi.org/10.1016/j.quascirev.2006.03.010>, 2006.
- 29 Martrat, B., Grimalt, J.O., Villanueva, J., van Kreveld, S., Sarntheim, M.: Climatic
30 dependence of the organic matter contributions in the north eastern Norwegian Sea over the
31 last 15,000 years, *Org. Geochem.*, 34, 1057-1070, [https://doi.org/10.1016/S0146-6380\(03\)00084-6](https://doi.org/10.1016/S0146-6380(03)00084-6), 2003.



- 1 Müller, J., Werner, K., Stein, R., Fahl, K., Moros, M., Jansen, E.: Holocene cooling
2 culminates in sea ice oscillations in Fram Strait. *Quaternary Science Reviews*, 47,1–14,
3 <https://doi.org/10.1016/j.quascirev.2012.04.024>, 2012.
- 4 Nilsen, F., Cottier, F., Skogseth, R., Mattson, S.: Fjord-shelf exchanges controlled by ice and
5 brine production: The interannual variation of Atlantic Water in Isfjorden, Svalbard, *Cont.*
6 *Shelf Res.* 28, 1838-1853, <https://doi.org/10.1016/j.csr.2008.04.015>, 2008.
- 7 Pawłowska, J., Lejzerowicz, F., Esling, P., Szczuciński, W., Zajączkowski, M., Pawłowski, J.:
8 Ancient DNA sheds new light on the Svalbard foraminiferal fossil record from the last
9 millennium, *Geobiology*, 12, 277-288, <https://doi.org/10.1111/gbi.12087>, 2014.
- 10 Pawłowska, J., Zajączkowski, M., Łacka, M., Lejzerowicz, F., Esling, P., Pawłowski, J.:
11 Palaeoceanographic changes in Hornsund Fjord (Spitsbergen, Svalbard) over the last
12 millennium: new insights from ancient DNA, *Clim. Past*, 12, 1459-1472,
13 <https://doi.org/10.5194/cp-12-1459-2016>, 2016.
- 14 Pawłowski, J., Holzmann, M., Berney, C., Fahrni, J., Cedhagen, T., Bowser, S.S.: Phylogeny
15 of allogromiid Foraminifera inferred from SSU rRNA gene sequences, *J. Foramin. Res.*, 32,
16 334-343, <https://doi.org/10.2113/0320334>, 2002.
- 17 Pawłowski, J., Esling, P., Lejzerowicz, F., Cedhagen, T., Wildings, T.A.: Environmental
18 monitoring through protest next-generation sequencing metabarcoding: assessing the impact
19 of fish farming on benthic foraminifera communities, *Mol. Ecol. Res.*, 14, 1129-1140, doi:
20 10.1111/1755-0998.12261, 2014a.
- 21 Pawłowski, J., Lejzerowicz, F., Esling, P.: Next-generation environmental diversity surveys
22 of foraminifera: Preparing the future, *Biol. Bull.*, 227, 93-106,
23 <https://doi.org/10.1086/BBLv227n2p93>, 2014b.
- 24 Piechura, J.: Dense bottom waters in Storfjord and Storfjordrenna, *Oceanologia*, 38, 285-292,
25 1996.
- 26 Polyakov, I. V., Pnyushkov, A.V., Alkire, M.B., Ashik, I.M., Baumann, T.M., Carmack, E.C.,
27 Goszczko, I., Guthrie, J., Ivanov, V.V., Kanzow, T.T., Greater role for Atlantic inflows on
28 sea-ice loss in the Eurasian Basin of the Arctic Ocean, *Science*, eaai8204,
29 <https://doi.org/10.1126/science.aai8204>, 2017.
- 30 Quadfasel, D., Rudels, B., Kurz, K.: Outflow of dense water from a Svalbard fjord into the
31 Fram Strait, *Deep Sea Res.*, 35, 1143-1150, [https://doi.org/10.1016/0198-0149\(88\)90006-4](https://doi.org/10.1016/0198-0149(88)90006-4),
32 1988.



- 1 Rasmussen, T.L., Forwick, M., Mackensen, A.: Reconstruction of inflow of Atlantic Water to
- 2 Isfjorden, Svalbard during the Holocene: Correlation to climate and seasonality, *Mar.*
- 3 *Micropaleontol.*, 94-95, 80-90, <https://doi.org/10.1016/j.marmicro.2012.06.008>, 2012.
- 4 Rasmussen, T.L., Thomsen, E., Skirbekk, K., Ślubowska-Woldengen, M., Klitgaard
- 5 Kristensen, D., Koç, N.: Spatial and temporal distribution of Holocene temperature maxima in
- 6 the northern Nordic seas: interplay of Atlantic-, Arctic- and polar water masses, *Quat. Sci.*
- 7 *Rev.*, 92, 280-291, <https://doi.org/10.1016/j.quascirev.2013.10.034>, 2014.
- 8 Rasmussen, T. L., Thomsen, E.: Brine formation in relation to climate changes and ice retreat
- 9 during the last 15,000 years in Storfjorden, Svalbard, 76-78°N, *Paleoceanography*, 29, 911–
- 10 929, <https://doi.org/10.1002/2014PA002643>, 2014.
- 11 Rasmussen, T.L., Thomsen, E.: Palaeoceanographic development in Storfjorden, Svalbard,
- 12 during the deglaciation and Holocene: evidence from benthic foraminiferal records. *Boreas*,
- 13 44, 24–44, <https://doi.org/10.1111/bor.12098>, 2015.
- 14 Reimer, P. J., Bard, E., Bayliss, A., Beck, J. W., Blackwell, P. G., Bronk Ramsey, C., van der
- 15 Plicht, J.: IntCal13 and Marine13 Radiocarbon Age Calibration Curves 0-50,000 Years Cal
- 16 BP. *Radiocarbon*, 55(4), 1869-1887, https://doi.org/10.2458/azu_js_rc.55.16947, 2013.
- 17 Risebrobakken, B., Moros, M., Ivanova, E.V., Chistyakova, N., Rosenberg, R.: Climate and
- 18 oceanographic variability in the SW Barents Sea during the Holocene, *The Holocene*, 20,
- 19 609-612, <https://doi.org/10.1177/0959683609356586>, 2010.
- 20 Róžańska, M., Poulin, M., Gosselin, M.: Protist entrapment in newly formed sea ice in the
- 21 Coastal Arctic Ocean, *J. Mar. Sys.*, 74, 887-901,
- 22 <https://doi.org/10.1016/j.jmarsys.2007.11.009>, 2008.
- 23 Rudels, B., Korhonen, M., Schauer, U., Pisarev, S., Rabe, B., Wisotzki, A.: Circulation and
- 24 transformation of Atlantic water in the Eurasian Basin and the contribution of the Fram Strait
- 25 inflow branch to the Arctic Ocean heat budget, *Prog. Oceanogr.*, 132, 128-152,
- 26 <https://doi.org/10.1016/j.pocean.2014.04.003>, 2015.
- 27 Sarnthein, M., Van Kreveld, S., Erlenkeuser, H., Grootes, P.M., Kucera, M., Pflaumann, U.,
- 28 Schulz, M.: Centennial-to-millennial-scale periodicities of Holocene climate and sediment
- 29 injections off the western Barents shelf, 75°N, *Boreas*, 32, 447-461,
- 30 <https://doi.org/10.1111/j.1502-3885.2003.tb01227.x>, 2003.
- 31 Sabbattini, A., Morigi, C., Negri, A., Gooday, A.J.: Distribution and biodiversity of stained
- 32 Monothalamous foraminifera from Tempelfjord, Svalbard, *J. Foramin. Res.*, 37, 93-106,
- 33 <https://doi.org/10.2113/gsjfr.37.2.93>, 2007.



- 1 Sabbattini, A., Bonatto, S., Bianchelli, S., Pusceddu, A., Danovaro, R., Negri A.:
2 Foraminiferal assemblages and trophic state in coastal sediments of the Adriatic Sea, *J. Mar.*
3 *Syst.*, 105, 163-174, <https://doi.org/10.1016/j.jmarsys.2012.07.009>, 2012.
- 4 Sabbattini, A., Nardelli M.P., Morigi C., Negri, A.: Contribution of soft-shelled
5 monothalamous taxa to foraminiferal assemblages in the Adriatic Sea, *Acta Protozool.*, 52,
6 181-192, <https://doi.org/10.4467/16890027AP.13.0016.1113>, 2013.
- 7 Skogseth, R., Haugan, P.M., Haarpaintner, J.: Ice and brine production in Storfjorden from
8 four winters of satellite and in situ observations and modeling, *J. Geophys. Res.*, 109, C10008,
9 <https://doi.org/10.1029/2004JC002384>, 2004.
- 10 Skogseth, R., Haughan, P.M., Jakobsson, M.: Watermass transformations in Storfjorden,
11 *Cont. Shelf Res.*, 25, 667-695, <https://doi.org/10.1016/j.csr.2004.10.005>, 2005.
- 12 Skogseth, R., Sandvik, A. D., Asplin, L.: Wind and tidal forcing on the meso-scale
13 circulation in Storfjorden, Svalbard, *Cont. Shelf Res.*, 27, 208-227,
14 <https://doi.org/10.1016/j.csr.2006.10.001>, 2007.
- 15 Smith, J.A., Hillenbrand, C-D., Pudsey, C.J., Allen, C.S., Graham, A.G.C.: The presence of
16 polynyas in the Weddell Sea during the Last Glacial Period with implications for the
17 reconstruction of sea-ice limits and ice sheet history, *Earth Planet. Sci. Lett.*, 296, 287-298,
18 <https://doi.org/10.1016/j.epsl.2010.05.008>, 2010.
- 19 Stuiver, M., Reimer, P.J.: Extended ¹⁴C database and revised CALIB 3.0 ¹⁴C age calibration
20 program, *Radiocarbon*, 35, 215-230, 1993.
- 21 Ślubowska-Woldengen, M., Rasmussen, T.L., Koç, N., Klitgaard-Kristensen, D., Nilsen, F.,
22 Solheim, A.: Advection of Atlantic Water to the western and northern Svalbard shelf since
23 17,500 cal yr BP. *Quat. Sci. Rev.*, 26, 463-478,
24 <https://doi.org/10.1016/j.quascirev.2006.09.009>, 2007.
- 25 Telesiński, M.M., Przytarska, J.E., Sternal, B., Forwick, M., Szczuciński, W., Łacka, M.,
26 Zajączkowski, M.: Palaeoceanographic evolution of the SW Svalbard shelf over the last
27 14 000 years, *Boreas*, 47, 410-422, <https://doi.org/10.1111/bor.12282>, 2018.
- 28 Thomsen, P.F., Willerslev, E.: Environmental DNA – An emerging tool in conservation for
29 monitoring past and present biodiversity, *Biol. Conserv.*, 183, 4-18,
30 <https://doi.org/10.1016/j.biocon.2014.11.019>, 2015.
- 31 Werner, K., Spielhagen, R.F., Bauch, D., Hass, H., Kandiano, E.S., Zamelczyk, K.: Atlantic
32 Water advection to the eastern Fram Strait – multiproxy evidence for late Holocene
33 variability. *Palaeogeogr. Palaeoclimatol. Palaeoecol.*, 308, 264-276,
34 <https://doi.org/10.1016/j.palaeo.2011.05.030>, 2011.



1 Winkelmann, D., Knies, J.: Recent distribution and accumulation of organic carbon on the
2 continental margin west off Spitsbergen. *Geochem. Geophys. Geosyst.*, 6, Q09012,
3 <https://doi.org/10.1029/2005GC000916>, 2005.

4 Wollenburg, J.E., Kuhnt, W.: The response of benthic foraminifers to carbon flux and primary
5 production in the Arctic Ocean, *Mar. Micropaleontol.*, 40, 189-231,
6 [https://doi.org/10.1016/S0377-8398\(00\)00039-6](https://doi.org/10.1016/S0377-8398(00)00039-6), 2000.

7

8 **Figures captions**

9 **Figure 1:** Study area and the location of the studied core ST_1.5 and the other cores discussed
10 in this paper.

11 **Figure 2:** Age–depth model of the studied core.

12 **Figure 3:** Sedimentological and micropaleontological data plotted versus age. The sediment
13 accumulation rate (SAR), mean grain size of the 0-63- μm fraction, ice-rafted debris (IRD)
14 flux and number of grains per gram of sediment, oxygen ($\delta^{18}\text{O}$) and carbon ($\delta^{13}\text{C}$) stable
15 isotopes in foraminiferal tests, the percentage of calcareous foraminifera individuals and the
16 flux and abundance of foraminifera are presented.

17 **Figure 4:** The abundance (expressed as the number of individuals per gram of dry sediment)
18 and the percentage of the dominant testate foraminifera.

19 **Figure 5:** The dominant components of the monothalamous assemblages. The abundance is
20 expressed as the percentage of the monothalamous sequences and the most abundantly
21 sequenced taxa are presented. The trend is indicated with the dashed line.

22 **Figure 6:** The percentage share of certain clades in the allogromiid sequences.

23 **Figure 7:** The percentage of sequences of dominant diatom taxa vs. time. The trend is
24 indicated with the dashed line.

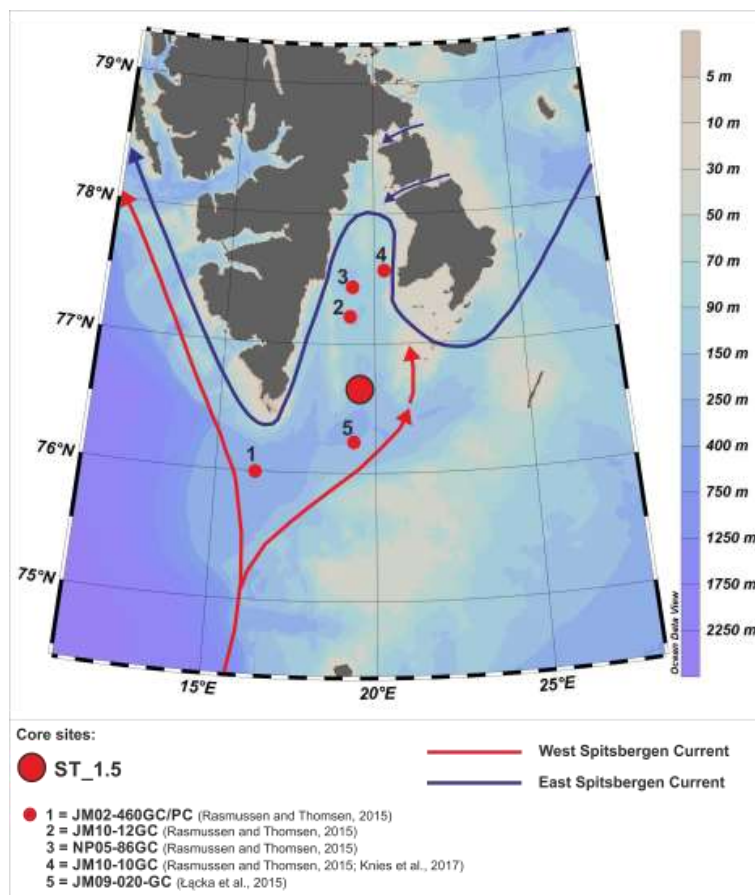
25

26 **Tables captions**

27 **Table 1:** Raw and calibrated AMS¹⁴C dates used in the age model.

28

29

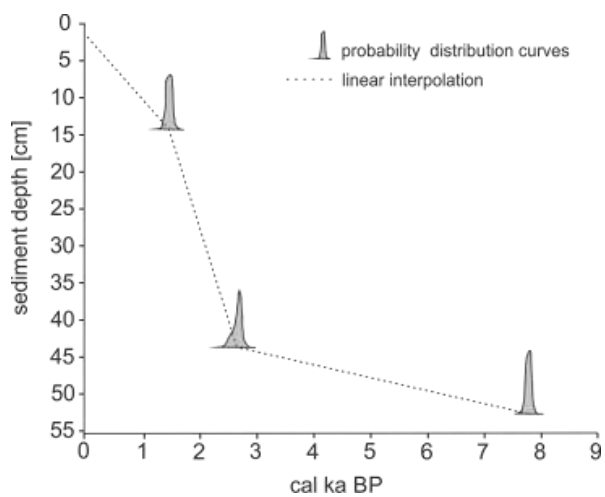


1

2 **Figure 1:** Study area and the location of the studied core ST_1.5 and the other cores discussed in this paper.

3

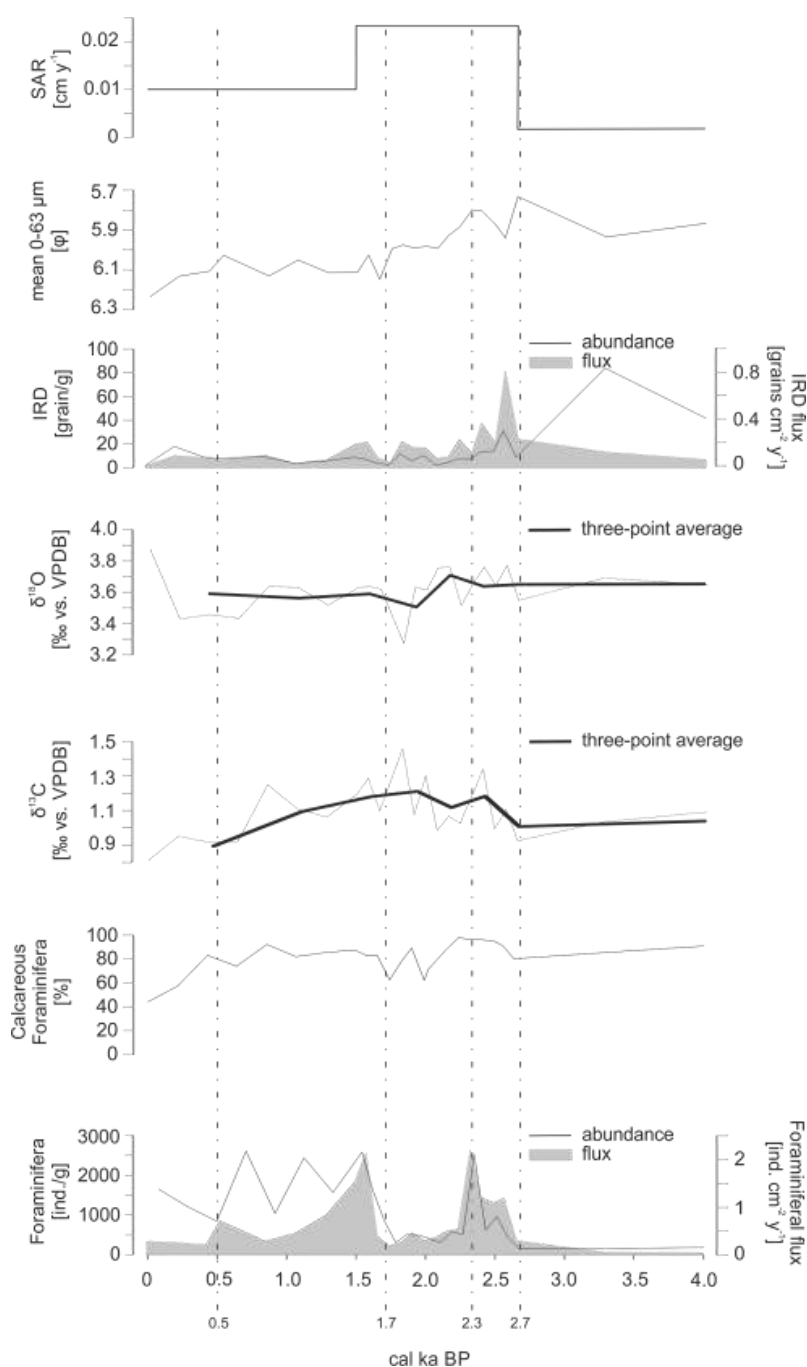
4



1

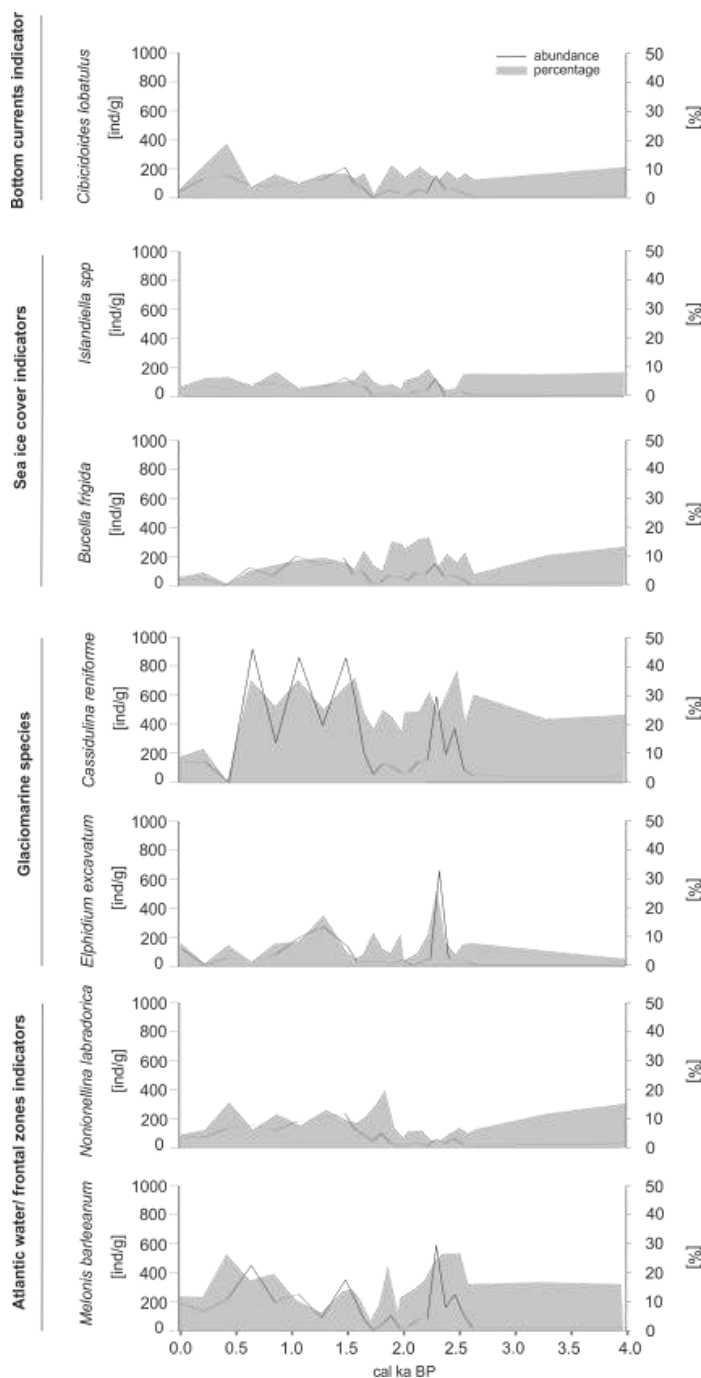
2 **Figure 2:** Age–depth model of the studied core.

3



1

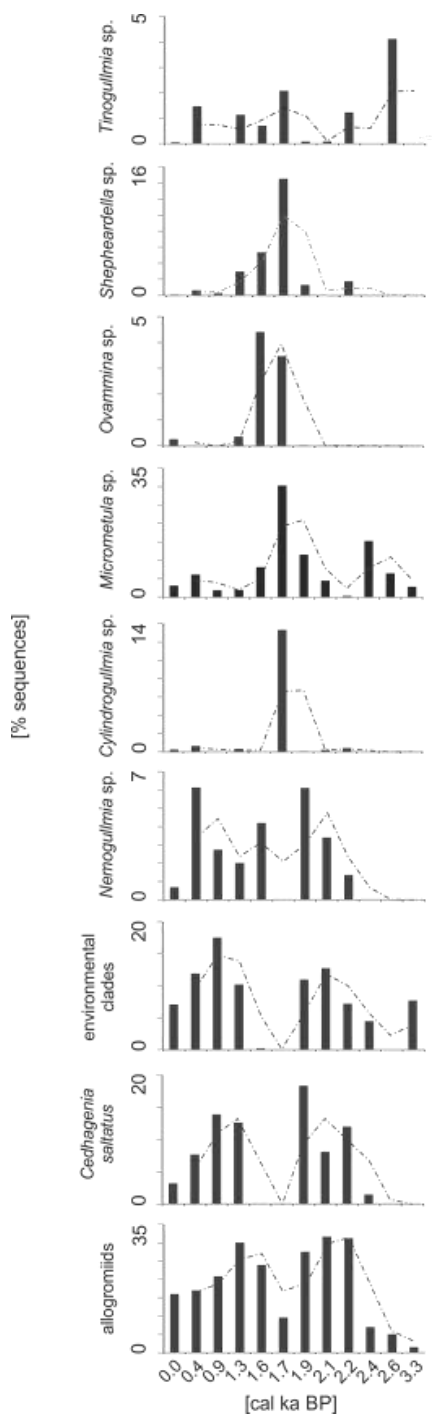
2 **Figure 3:** Sedimentological and micropaleontological data plotted versus age. The sediment accumulation rate
3 (SAR), mean grain size of the 0-63- μm fraction, ice-rafted debris (IRD) flux and number of grains per gram of
4 sediment, oxygen ($\delta^{18}\text{O}$) and carbon ($\delta^{13}\text{C}$) stable isotopes in foraminiferal tests, the percentage of calcareous
5 foraminifera individuals and the flux and abundance of foraminifera are presented.



1

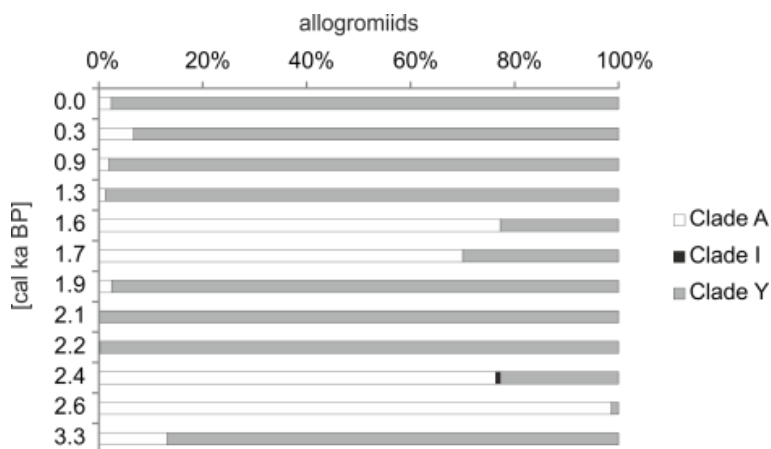
2 **Figure 4:** The abundance (expressed as the number of individuals per gram of dry sediment) and the percentage
3 of the dominant testate foraminifera.

4



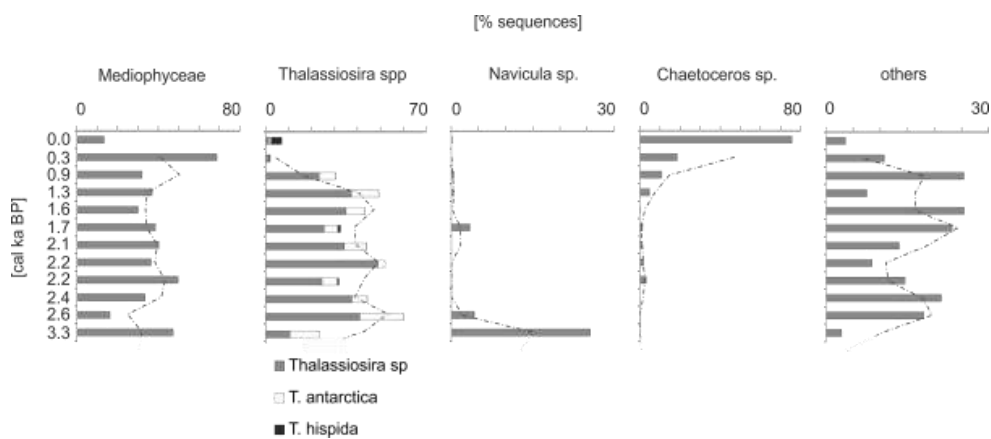
1

2 **Figure 5:** The dominant components of the monothalamous assemblages. The abundance is expressed as the
 3 percentage of the monothalamous sequences and the most abundantly sequenced taxa are presented. The trend is
 4 indicated with the dashed line.



1
2
3
4
5
6
7

Figure 6: The percentage share of certain clades in the allogromiid sequences.



8
9

Figure 7: The percentage of sequences of dominant diatom taxa vs. time. The trend is indicated with the dashed line.

10
11
12
13
14
15
16



1 **Table 1:** Raw and calibrated AMS¹⁴C dates used in the age model.

Sediment depth [cm]	Material (shells)	Raw AMS ¹⁴ C	Calibrated years BP ± 2σ	Cal. a BP used in age model
2.5	<i>Nuculana pernula</i>	107.38 ± 0.33 pMC	-	-
5.5	<i>Yoldiella lenticula</i>	290 ± 30 BP	-	-
14.5	<i>Turitella erosa</i>	2020 ± 30 BP	1356-1555	1500
43.5	<i>Yoldiella solituda</i>	3010 ± 50 BP	2484-2787	2700
52.5	<i>Yoldiella lenticula</i>	7545 ± 35 BP	7803-7989	7890

2